Natural and Anthropogenic Changes to the Dissolved Inorganic Carbon System in the Western Equatorial Pacific During the Last Three Decades

Tony Dominguez-Giron

University of Washington, Seattle, WA

School of Oceanography

tjdom20@uw.edu

June 2, 2023

Abstract

The Western Pacific is a relatively unstudied area that is important for the climate because it is influenced not only by natural processes such as El Niño Southern Oscillation (ENSO) and seasonal variability but also the anthropogenic forces. The ocean's Dissolved Inorganic Carbon system (DIC), or carbonate system, is essential for how the ocean functions because of the complex air-sea interactions at the equator. The DIC system consists of the total carbon in the ocean that keeps the ocean's chemical balance in equilibrium. The changes in DIC were determined using measurements from three cruises from 2023, 2007, and 1993 with a similar transect along the Western Equatorial Pacific. Between 1993 and 2023, the ΔDIC in the 30 years was the highest near the equator (northward). This ΔDIC concentration was limited to mostly the upper 100 meters with a 200 μmol/kg increase between 1993 and 2023. The most significant DIC increase was seen above the thermocline during each cruise. A quasi-linear relationship exists between the DIC concentration during each cruise and the respective atmospheric carbon dioxide measurement from Mauna Loa Observatory. This study concludes that despite the Western Equatorial Pacific being a region of air-sea flux of CO_2 from the ocean to the atmosphere, the DIC values have continue to increase. DIC is also influenced by changes in air-sea gas exchanges that result from ENSO and seasonal variability during each cruise.

Plain Language Summary

The goal of this study is to seek a correlation between changes in the carbon system, known as the Dissolved Inorganic Carbon (DIC) system, in the Western Equatorial Pacific and natural processes such as periods of El Niño Southern Oscillation (ENSO) and the changing seasons as well as the addition of carbon dioxide to the atmosphere. The DIC system is crucial because it informs how the input and output of carbon impact the ocean's carbon system. The

DIC concentration was compared for 2023, 2007, and 1993. Over the 30 years, the highest ΔDIC concentration, 200 μmol/kg, was observed in the upper 100 meters and north of the equator. During each cruise, the most significant ΔDIC were limited to above 200 meters. The DIC concentrations were also found to have an increasing linear relationship with carbon in the atmosphere from the Mauna Loa Observatory, located in Hawaii. The results of this study indicate that the DIC concentration in the Western Equatorial Pacific is increasing due to the ocean in that region being a sink for human-emitted carbon, in addition to being influenced by naturally occurring processes, such as ENSO and seasonal variability. Long-term records of this understudied region are necessary to assess better the impact that human emissions will have on the DIC system and naturally occurring processes in the future.

Introduction

The ocean is crucial in regulating atmospheric carbon dioxide (CO_2) and storing anthropogenic carbon in the shallower water. As of 2020, atmospheric CO_2 levels were above 410 ppm, almost 50% more than pre-industrial levels, a rate increase that has not been observed in the last 55 million years of the geologic record (Doney et al., 2020). There is a seasonal variation of atmospheric CO_2; however, the atmospheric CO_2 is expected to continue to increase with anthropogenic carbon sources in the atmosphere (Figure 1) (*Monthly Average*, n.d.). Anthropogenic carbon results from the addition of inorganic carbon that impacts the air-sea gas exchange system due to carbon emissions to the atmosphere; Some of the significant anthropogenic carbon sources include burning fossil fuels, deforestation, and cement production (Gruber et al., 2019). Globally, humans emit approximately 10 Pg C per year, and 50% of that remains in the atmosphere (Carter et al., 2019). The ocean has taken up approximately 24% of

the total cumulative anthropogenic carbon since the beginning of the pre-industrial age (1850-2019) (Middelburg et al., 2019).

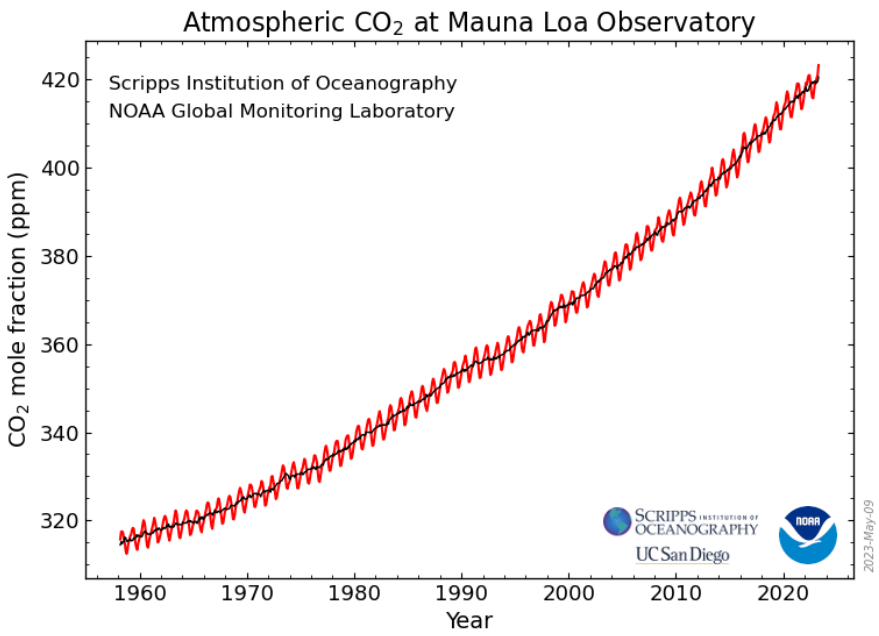

Figure 1- Atmospheric CO_2 concentrations measured from Mauna Loa Observatory. The increasing trend dates to more than five decades. Retrieved from NOAA (https://gml.noaa.gov/ccgg/trends/)

Each ocean basin varies in its ability to uptake and store anthropogenic carbon. Carter et al. (2019) state that the Atlantic Ocean is more efficient at storing anthropogenic carbon than the Pacific Ocean due to the North Atlantic Deep-Water Formation (NADW) region in which deep Atlantic waters have been exposed to the atmosphere on timescales of hundreds of years. The opposite is true for the Pacific Ocean, where deep Pacific waters have not had atmospheric interaction on timescales of thousands of years. About 30% of the anthropogenic carbon is confined to the thermocline, typically at shallower depths above 200 meters (Sabine et al., 2004). Another study conducted from 1994 to 2007, involving the extended multiple linear regression (eMLR) method, found that 50% of the anthropogenic carbon signal can be found in the upper 400 meters, and the signal decreases exponentially with depth (Gruber et al., 2019). While some

regions of the ocean equilibrate with atmospheric CO_2, other regions, such as the Equatorial Pacific, are complex and sensitive to anthropogenic carbon.

This region is relatively under sampled for the purposes of resolving the complex ocean dynamics in the Equatorial Pacific. The Equatorial Pacific is a critical and unique region of the world because of the various natural oceanographic processes occurring at this location. For example, the Equatorial Pacific is a region of divergence resulting from complex wind dynamics. As divergence occurs at the equator, old nutrient-rich waters are upwelled from the deep to the surface (Sutton et al., 2014). These waters are rich in CO_2 due to respiration, creating anomalies in the air-sea gas exchange and the carbonate system. In regions where strong vertical and horizontal transport of DIC-rich waters result in elevated nutrient concentrations that exceed net biological export, such as the Equatorial Pacific, there tends to be a biological CO_2 supersaturation; therefore, the ocean loses CO_2 to the atmosphere (Keeling et al., 2004).

DIC, or Total CO_2, is the total inorganic carbon dissolved in seawater, mostly comprised of bicarbonate and carbonate ions (Pimenta & Grear, 2018). DIC is the sum of carbonic acid, bicarbonate, and carbonate ions. The following equation explains the total inorganic carbon in the carbonate system (Bates et al., 2014):

$$\mathbf{DIC = [H_2CO_3] + [HCO_3^-] + [CO_3^{2-}]}$$

Figure (2) illustrates the various sources contributing to and impacting the carbonate system. Five processes that control the carbon cycle are air-sea gas exchange, net primary production, vertical diffusion, horizontal transport, and vertical entrainment of inorganic carbon during seasonal changes when the mixed layer deepens (Keeling et al., 2004).

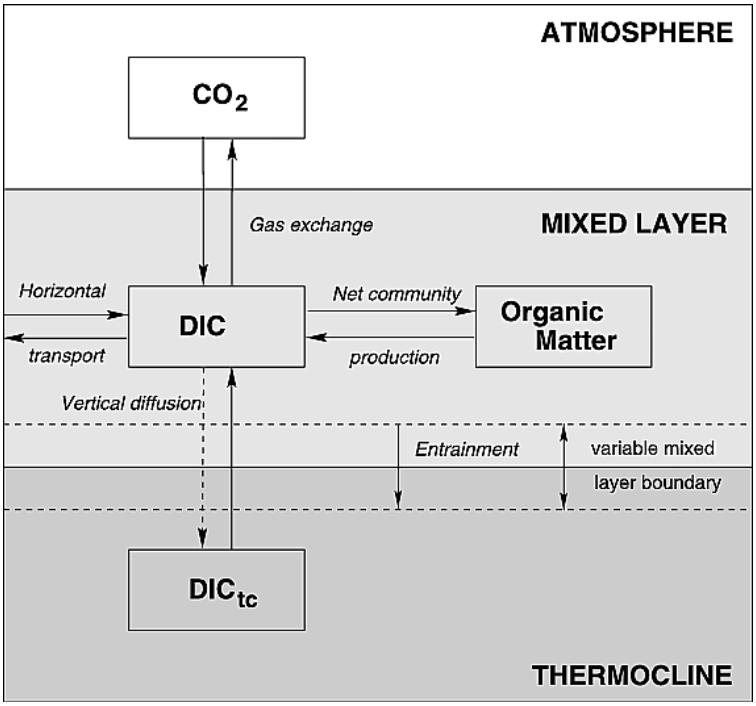

Figure 2. Oceanic carbon pools and the various contributors within the mixed layer and thermocline. Some major processes depicted are air-sea gas exchange, net primary production, vertical diffusion, entrainment, etc. Figure from Keeley et al (2004).

When CO_2 enters the ocean, the CO_2 dissolves in seawater (forming carbonic acid); CO_2 impacts the acid-base chemistry that changes the speciation of dissolved ions resulting in a decrease of the seawater pH due to the increase of hydrogen ion concentration (H+) (Doney et al., 2020). Since the preindustrial era, the surface ocean pH is estimated, on average, to have decreased by about 0.1 units globally with increasing anthropogenic CO_2 and a decline in carbonate ion concentration, which correlates to approximately a 30% increase in H+ ion concentration (Doney et al., 2020). As CO_2 increases in the ocean, declining carbonate ion concentration and declining pH in the ocean are contributing to ocean acidification, a process that results in a corrosive environment for calcifying organisms in need of calcium carbonate ($CaCO_3$) minerals for shell building (Carter et al., 2019).

Ocean acidification results from the changing ocean properties that impact calcifying organisms and other marine life. More specifically, ocean acidification is the collective result of

increasing pCO_2 and a reduction in pH and carbonate ion concentration (Landschützer et al., 2018). Increasing the atmospheric CO_2 by two times the preindustrial levels will result in approximately a 30% decrease in carbonate ion concentration and a 60% increase in hydrogen ion concentration if the surface ocean pCO_2 continues to increase proportionally to anthropogenic CO_2 in the atmosphere (Sabine et al., 2004). The pCO_2 depends on seasonal variability, which is dependent on natural oceanographic processes and anthropogenic carbon. For example, increasing primary production from winter to summer months results in DIC uptake, which correlates to a decrease in pCO_2 during this seasonal change (Takahashi et al., 2014).

Anthropogenic carbon complicates an already complex DIC system influenced by naturally occurring processes. For example, the warm and cold phases of El Niño Southern Oscillation (ENSO) cycles determine the strength of upwelling along the equator, impacting rainfall and weather worldwide (Sutton et al., 2014). Sutton et al. (2014) state that the Equatorial Pacific supplies the largest natural source of CO_2 to the atmosphere during La Niña events, resulting from the persistency of easterly trade winds that upwell waters enriched in CO_2. More specifically, more carbon outgasses into the atmosphere during La Niña events and less carbon outgasses into the atmosphere during El Niño events.

Understanding the various sources of natural and anthropogenic carbon sources can provide us with historical climate patterns and make predictions of future climate and changes to the carbonate system. National Oceanic and Atmosphere Administration (NOAA) provides a monthly history of the ENSO events and their intensities from 1979 (Figure 3). NOAA does this by using a time series of five variables that include sea level pressure, sea surface temperature,

surface wind for both zonal and meridional components, and outgoing longwave radiation over the tropical Pacific Ocean (30S-30N and 100E-70W) (*Multivariate ENSO*, n.d.).

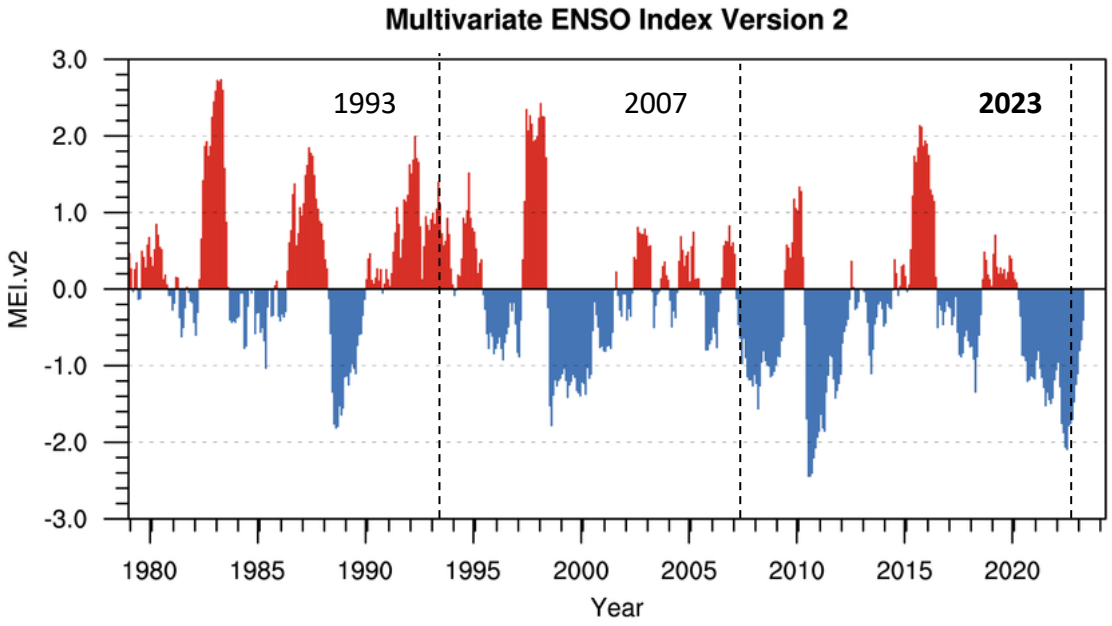

Figure 3. NOAA provides the past and current periods of the ENSO and their intensity. The year dates back from 1979 on the X-axis to the current year, 2023. The intensity of the ENSO events, Multivariate ENSO magnitude of -3.0 to 3.0, is displayed on the on the Y-axis. A MEI.v2 magnitude of 3.0 (Red) would correlate to the strongest magnitude of El Niño and -3.0 is correlated to the strongest La Niña periods. Each dashed line identifies the time when each cruise occurred. Retrieved and modified from https://psl.noaa.gov/enso/mei/

The complex variations of the carbonate system can be observed through measurements of total alkalinity and pH. Total alkalinity is a conservative and measurable property that informs us about the number of hydrogen proton donors and acceptors in seawater (Sutton et al., 2014). We can determine cation, ion, and hydrogen concentrations by measuring alkalinity. When CO_2 enters the ocean, it dissociates into bicarbonate or carbonate ions and releases hydrogen protons (Pimenta & Grear, 2018). Pimenta & Grear (2018) state that the release of H+ protons increase

the concentration and decreases the pH (pH = -log(H)). Alkalinity and pH measurements help determine natural or anthropogenic shifts in the carbonate system.

Methods

The Research Vessel (R/V) Thomas G. Thompson departed Honolulu, Hawaii, USA, and began transit to Suva, Fiji. A total of 16 stations were visited for data collection, of which only 11 stations were used for this study (Figure 4). Ocean properties were measured between March 3-7, 2023. The DIC values of the 2023 cruise were compared to two other cruises that visited the same transect within the last 30 years. The first cruise, also aboard the R/V Thompson, visited the transect between July 05-September 23, 1993. The second cruise, completed by the R/V MIRAI, visited the transect between November 22-December 26, 2007. During the 2023 cruise, deployment of oceanic instrumentation was limited to shallower depths relative to the previous two cruises. As a result, only the upper 1100 meters are considered for this study.

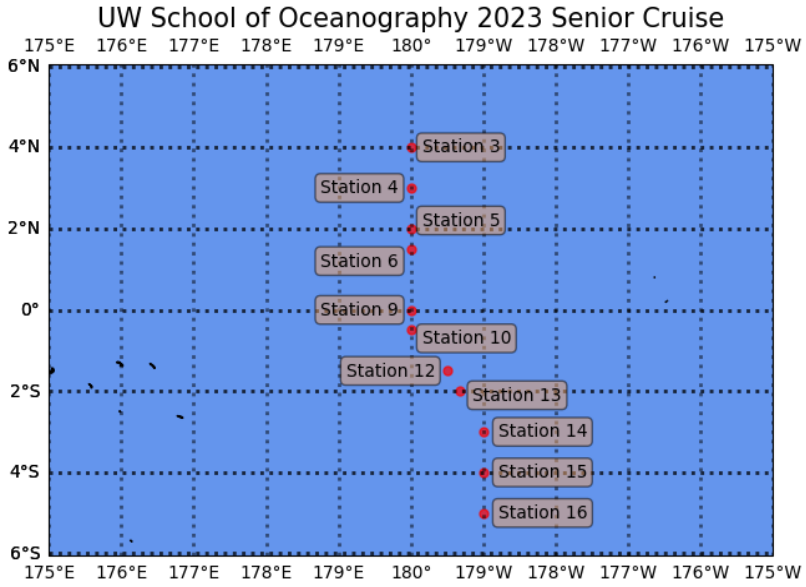

Figure 4. Ocean properties were measured at 11 of 16 stations for the purposes of calculating DIC concentration.

Alkalinity and pH were measured using the Mettler-Toledo T5 auto-titrator with a 9-sample carousel. The pH measurements were collected in-situ using the SeaBird 911 plus

conductivity, temperature, and depth (CTD) fitted with a Clark electrode. The Mettler-Toledo T5 auto-titrator was calibrated to Batch 204 standards dated July 22, 2022, retrieved from the NOAA website (*Information on Batches*, n.d.). Alkalinity values were used in conjunction with pH values to calculate DIC concentration. CO2SYS, a website, was utilized to calculate the DIC concentration of seawater. CO2SYS can calculate CO_2 in seawater or freshwater using two of four water properties, such as total alkalinity (TA) and pH (Lewis & Wallace, 1998). Within CO2SYS, the following parameters were selected: **Set of Constants**= *K1, K2 from Merbach et al. 1973 refit by Dickson & Millero,1987*, **KHSO4**= *Dickson*, **pH Scale** = *Total Scale (*μmol/kgSW*)*, and **[B]I Value**= *Uppstrom,1974*.

DIC values for the 2023 cruise were calculated from CO2SYS and manipulated using Ocean Data View (ODV), a software package, and via Python coding. The data for the three cruises were used to create a grid of latitudes between 5N° to 5S° with a depth of 1100 meters. Grids were created to generate plots illustrating the difference in DIC between the current data and each previous cruise's gridded data using the data from the three cruises. Generating the previously mentioned plots was crucial to observe changes in the DIC system and linking those changes to periods of ENSO patterns, seasonal variability, and changes deriving from anthropogenic carbon. Based on the DIC concentration across the three datasets, one should understand the major driving forces influencing DIC in the upper 1100 meters.

Results

The pH values in the water column have a consistent and predictable profile compared to the alkalinity values (Figure 5A). Near the surface, higher pH values range between approximately 8.18 to 8.25. Below 200 meters, there is more variability in the pH values as they become more acidic with depth. pH values ranging from approximately 7.6 to 7.75 can be

observed below 1000 meters. The alkalinity values, however, have more variability at the surface and depth (Figure 5B). At the surface, the alkalinity values range from 2330 μmol/kg to nearly 2400 μmol/kg. The highest variability in alkalinity data is in the upper 200 meters. Below 200 meters there is a slight trend of increasing alkalinity with depth.

A **B**

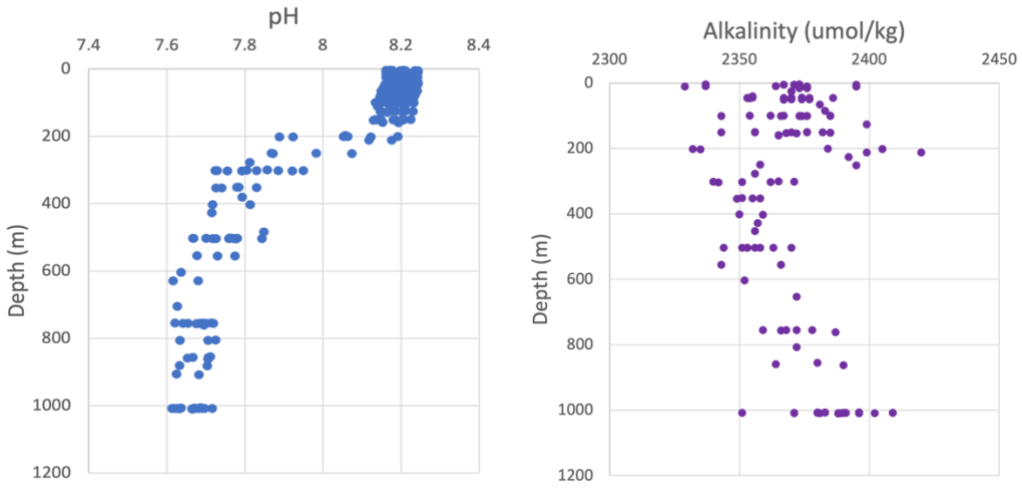

Figure 5. Panel A: pH values from the pH Scale on the X-axis versus depth(m) on the Y-axis in the water column for 2023 Senior Cruise. Panel B: Alkalinity (µmol/kg) values on the X-axis versus depth (m) on the Y-axis in the water column for 2023 Senior Cruise.

The pH and alkalinity values were used to calculate DIC through the CO2SYS software. The 2023 DIC profile is compared to the two previous cruises (Figure 6). Using gridded data for the three DIC profiles allows for a general comparison in the upper 1100 meters of the water column. Among the three DIC profiles, the most significant changes in DIC are observed at the surface. The three sets of data have similar profiles with an increasing DIC concentration with increasing depth. The 1993 DIC profile ranges from approximately 1900 μmol/kg to about 2300 μmol/kg. The 2007 DIC profile ranges from approximately 2000 μmol/kg to similar DIC values as the 1993 cruise with increasing depth. Lastly, the 2023 DIC profile ranges from about 2100

μmol/kg to an average of 2300 μmol/kg but the 2023 DIC profile certainly has some DIC concentration values above 2300 μmol/kg.

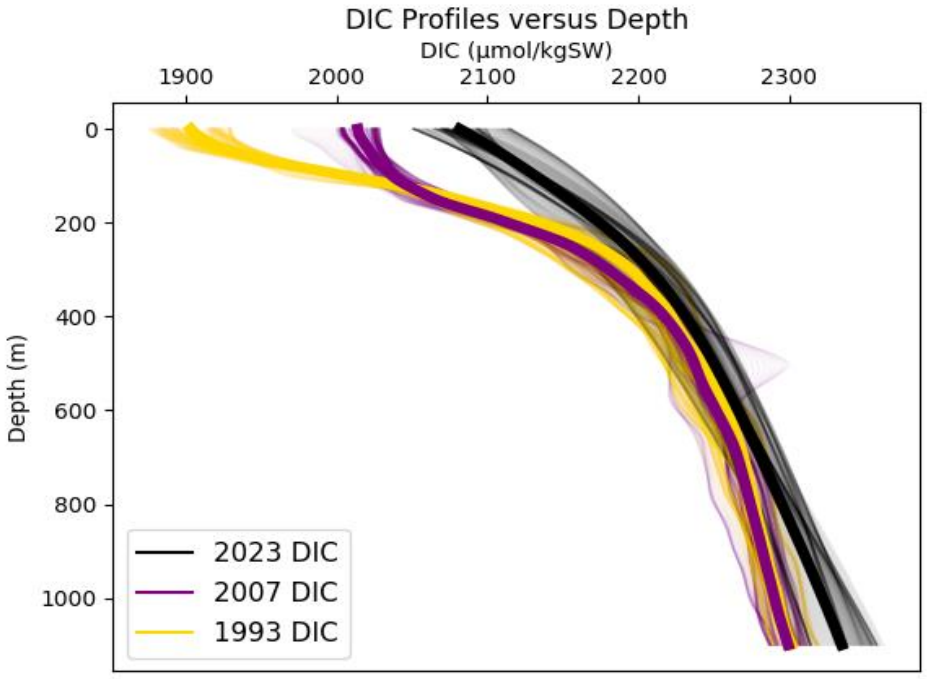

Figure 6. DIC Profiles for 1993, 2007, and 2023 cruises. The profiles are for the upper 1100 meters for latitudes 5N° to 5S°.The thick same-colored lines represent the average DIC concentration at that depth. The lighter portion of the profiles represent the range of DIC concentration at each depth .

The DIC concentrations from the upper 1100 m between 5N and 5 S from the three cruises were gridded using ODV (Figs. 7) to identical x-y grids. The changes in DIC between the cruises (Fig. 8) was calculated by subtracting one grid from the other. In 1993, the lowest values of DIC, 1900 μmol/kg, were limited to the upper 100 meters and increased gradually to 2300 μmol/kg at 1100 meters (Figure 7A). The same is true for the 2007 cruise in which values of approximately 2000 μmol/kg can be observed at the upper 100 meters and steadily increase to 2300 μmol/kg at 1100 meters across latitudes (Figure 7B). Lastly, the 2023 cruise illustrates an increase in DIC concentration that ranges from 2300 μmol/kg in the upper 100 meters to about 2400 μmol/kg at a depth of 1100 meters (Figure 7C).

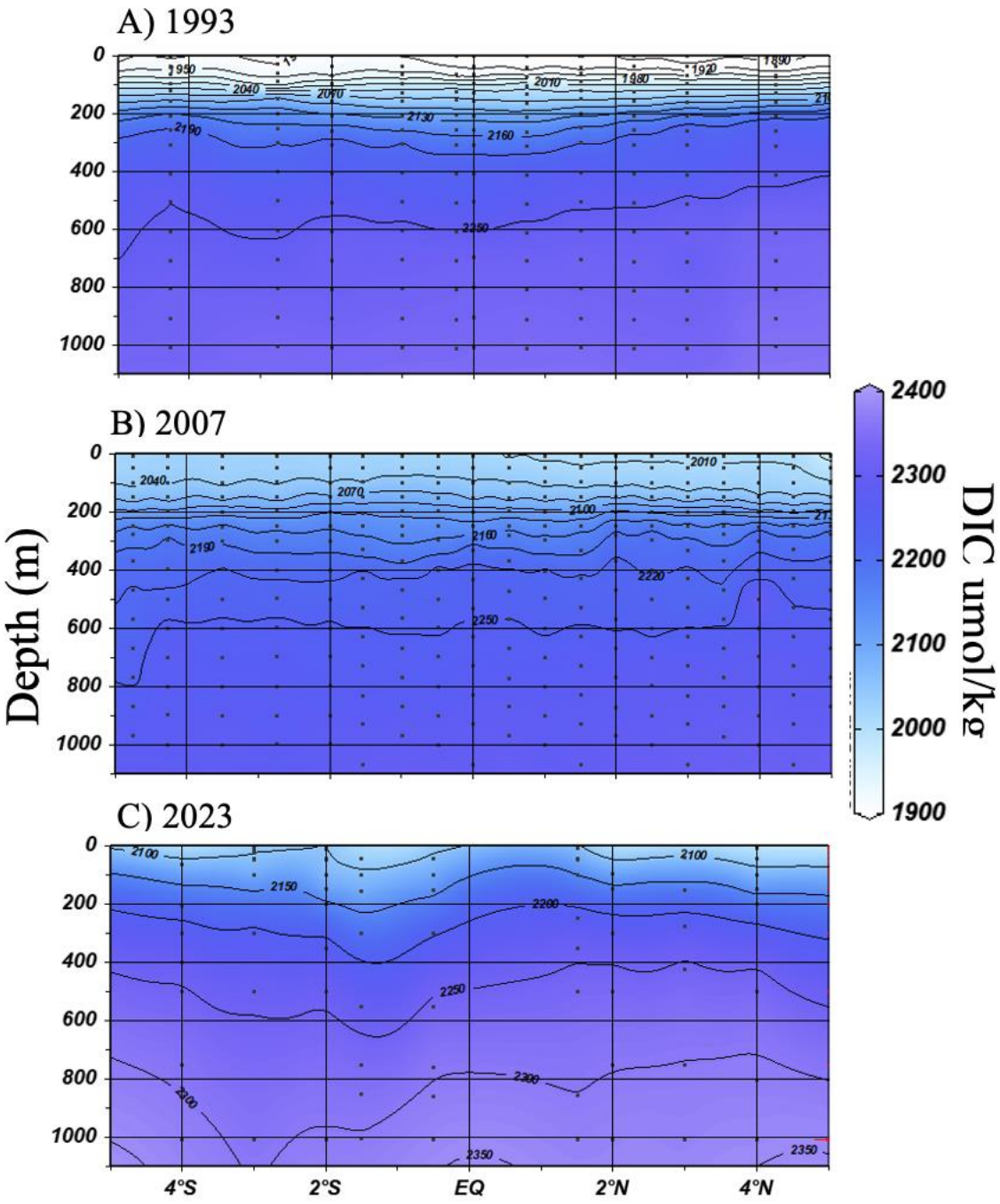

Figure 7. Vertical section of DIC measurements for the upper 1100 meters of the water column. Contour plots are for the R/V Thompson and the R/V Mirai's transects between 5N° to 5S°. *Latitude is on the lower axis and depth is on the left-most vertical axis. A) R/V Thompson's transect between July 05, 1993 and September 02, 1993. B) R/V Mirai's transect between November 22, 2007 and December 26, 2007. C) R/V Thompson's transect from March 03-07 2023.*

To analyze where the ΔDIC has occurred in the water column, each grid was subtracted from each other to determine changes in DIC between cruises for the upper 1100 meters (Figure 8). The grid from the 1993 cruise was subtracted from the 2007 cruise (Figure 8A). Figure 8A was created as a quality check to verify the validity of the data and to gauge and predict patterns of ΔDIC over 30 years between 1993 and 2023. There was almost no increase in DIC concentration at the depth greater than approximately 150 meters. Although there are light-colored portions at depth greater than 150 meters, there is no significant ΔDIC. The most noticeable ΔDIC from 1993 to 2007 occurred in the upper 150 meters and ranges from 40 μmol/kg to 80 μmol/kg.

Between 2007 and 2023, the DIC concentration increased in the upper 200 meters of the water column (Figure 8B). During these 16 years, the ΔDIC for the upper 200 meters ranges from 75 μmol/kg to 105 μmol/kg. The most significant ΔDIC, 105 μmol/kg, is seen north of the equator. Below the thermocline of approximately 200 meters, an increase ranging from 15 μmol/kg to 45 μmol/kg is observed from 5N° to 5S° for the remaining 900 meters of the water column. Significant changes are observed over the 30-year period (Figure 8C). The largest ΔDIC occurs in the upper 200 meters of the water column over 30 years. There are two patches in the water column below the thermocline where ΔDIC is seen to decrease at depth lower than the thermocline but relatively low ΔDIC compared to the upper 200 meters. The ΔDIC indicates an increase in DIC concentration from 1993 to 2023 ranging from 50 μmol/kg to 200 μmol/kg with the highest ΔDIC occurring just north of the equator.

A

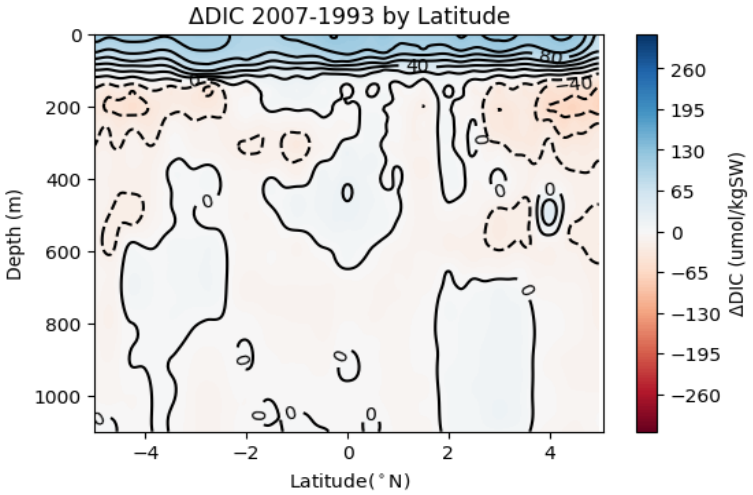

B

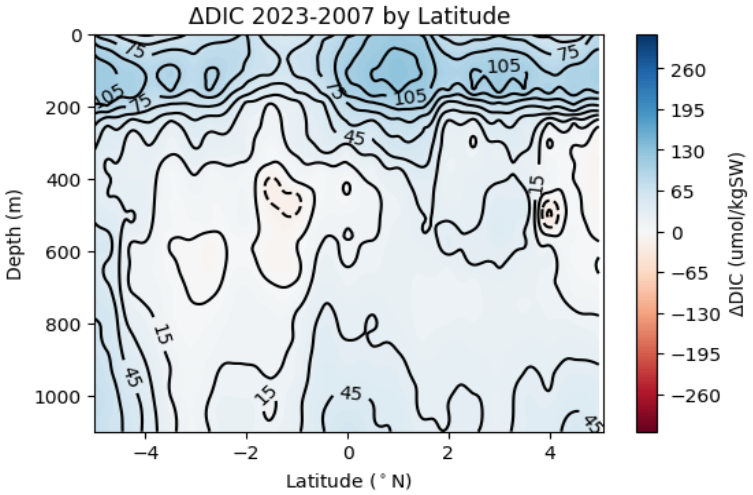

C

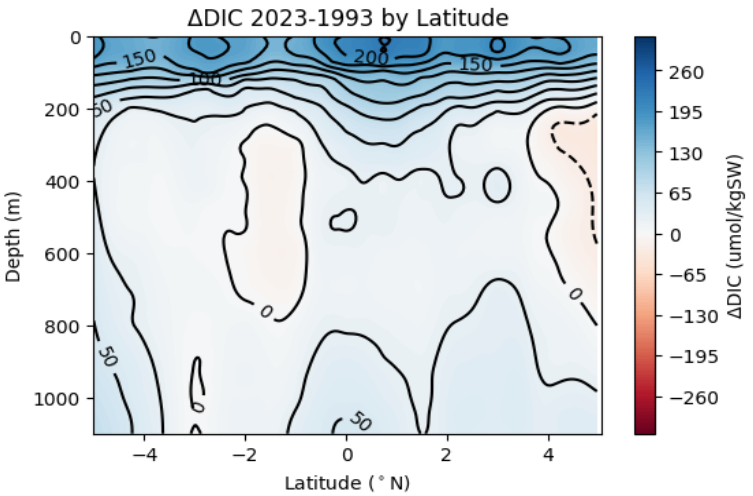

Figure 8. Vertical shifts of the DIC concentration over the last three decades. Latitudes 5N° to 5S° are displayed on the X-axis. Depth ranging from the surface to 1100 meters are displayed on the Y-axis. The color bar is the ΔDIC concentrations. The blue colors indicate an increase in DIC, the red color indicate a decrease in DIC, and white colors indicate no change in DIC. Panel A: ΔDIC change from 1993 to 2007. Panel B: ΔDIC change from 2007 to 2023. Panel C: ΔDIC change from 1993 to 2023.

The average surface DIC concentrations, μmol/kg, from Figure 6 were then plotted against the atmospheric CO_2, ppm, from Figure 1 for the year of each respective cruise (Figure 9). In 1993 the atmospheric CO_2 was 355 ppm which correlates to a DIC concentration of 1900 μmol/kg. For the intermediate cruise, 2007, the atmospheric CO_2 increased to 383 ppm while the average surface DIC concentration increased to 2010 μmol/kg. Lastly, there was an average increase of average surface DIC concentration and atmospheric CO_2 of approximately 70 μmol/kg and 40 ppm, respectively during the 2023 cruise.

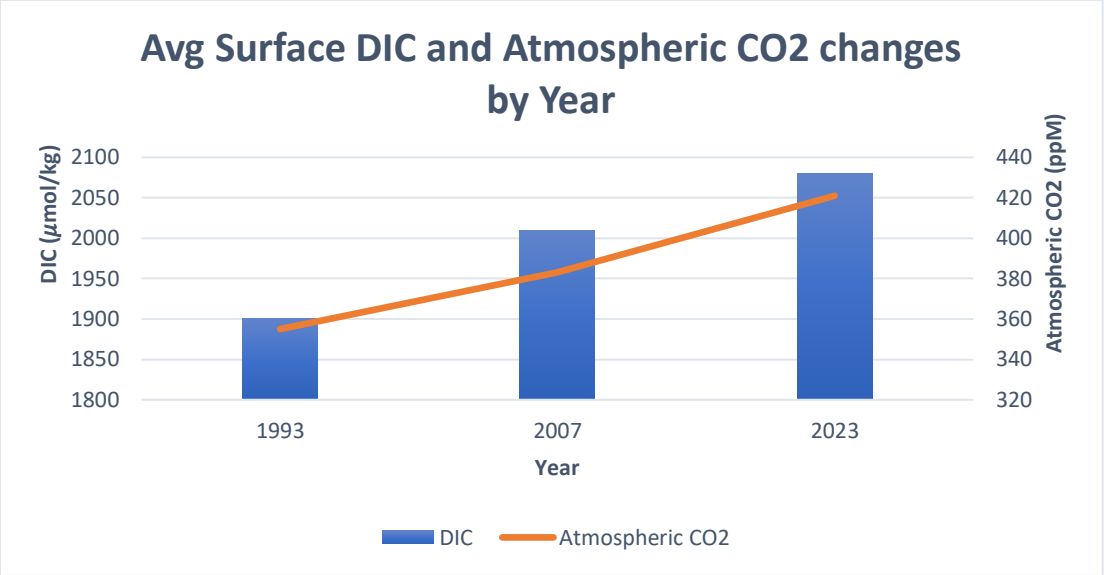

Figure 9- The relationship between atmospheric CO_2 and average DIC concentration at the surface.

Discussion

The pH values at the surface are consistent with the standard pH range (Figure 5A). In surface waters, pH ranges from 8.1 to 8.2, but the uptake of anthropogenic carbon can potentially alter the carbon system's chemical equilibrium (Bates et al., 2014). Compared to oligotrophic parts of the ocean, pH in the equatorial Pacific is highly variable (Sutton et al., 2014). The pH values at the surface could correlate to primary production occurring at the surface. Increased primary production converts DIC to organic carbon which would increase pH, whereas lower

primary production rates result in a more acidic pH. Extreme mixing, which leads to an elevated nutrient concentration and increased primary production rates, results in lower DIC concentration due to higher consumption of carbon (Merlivat et al., 2018). In contrast, the lower pH values at depth could be correlated to increased net respiration. At the surface, pH depends on DIC concentration and alkalinity, both controlled by physical and biological processes; however, DIC also depends on the air-sea gas exchange (Takahashi et al., 2014). Additionally, as the DIC concentration increases with depth, the pH lowers due to net respiration from organisms exceeding primary production. More acidic pH values and higher hydrogen proton (H+) concentration are closely related to higher DIC concentration. Seasonal variability, ENSO, and anthropogenic carbon in the atmosphere influence changes in DIC concentration.

Seasonal Variability

All cruises occurred during different months of the year, which indicate that seawater properties were influenced to an extent by the seasonal variations among the cruises and therefore impacted DIC concentrations over the 30 years. In 1993, the cruise occurred during the summer months (July-Sept), which means that warmer conditions were more than likely present. The 2007 and 2023 cruises occurred in November-December and early March, respectively. These winter months will bring colder temperatures that will impact biological production and gas solubility, two significant ocean properties that influence DIC concentration. DIC concentration is higher during winter months and lower in summer months, reflecting the upward mixing of deep rich- CO_2 and increased primary production, respectively (Takahashi et al., 2014). Horizontal transport, vertical transport, and mixing processes greatly impact the seasonal variability of DIC concentration; however, it still needs to be understood how to distinguish contributions between each process (Keeling et al., 2004). Although seasonal temperature shifts

are driving significant processes in the ocean that influence DIC concentrations, the magnitude of seasonal variability is controlled by periods of ENSO.

ENSO

The ΔDIC (Figure 8) indicates that ENSO periods at the equator may influence the DIC concentration in the upper 1100 meters. The Multivariate ENSO Index (MEI) (Figure 3) supports that ΔDIC in the upper 1100 meters could result from ENSO periods. For the 1993 cruise, NOAA reports an MEI magnitude ranging from 0.6 to 0.9 for the July to September cruise. These values correlate to a warm, moderate period of El Niño where warmer temperatures are expected, additional warming to the summer season. One must also consider that Figure 3 reveals at least three El Niño events before 1993, which may amplify ocean properties via positive feedback, such as warmer-than-usual temperatures. During El Niño, there is a considerable reduction of carbon supply at the surface due to downwelling patterns caused by wind dynamics, which ultimately lower the pCO_2 and decrease the CO_2 outgassing to the atmosphere (Mogollón, 2020). Warmer temperatures would not only shoal the thermocline but also decrease gas solubility. There is also generally less upwelling during El Niño periods, which could be a limiting factor for primary production due to less carbon/nutrients being upwelled. Furthermore, during El Niño events, we should expect to see warmer temperatures above the thermocline, which would also decrease the CO_2 concentration, due to decreased gas solubility, in regions of the water column where temperature increases.

The 2007 cruise occurred from November to December, correlating to MEI magnitudes of -1.2 to -1.3. These values indicate a relatively colder period of La Niña compared to the 1993 cruise. However, Figure 3 suggests that the 2007 cruise occurred during a transition between El Niño and La Niña events. During La Niña, higher concentrations of DIC are present in the upper

180 meters of the water column compared to the 1993 cruise (Figure 8A). During El Niño, the increasing surface temperatures decrease DIC concentrations due to reduced CO_2 solubility (Mogollón, 2020). The opposite is true for La Niña events. Below the thermocline of 180 meters, however, there is a slight negative ΔDIC which suggests that the DIC concentration decreased from 1993 to 2007. This negative ΔDIC could be explained by the early stages of La Niña, in which colder temperatures brought by La Niña have been limited to the thermocline and will therefore limit major gas solubility changes to depths above the thermocline.

Higher ΔDIC are expected between the 2007 and 2023 cruises for the upper 1100 meters relative to 1993 to 2007 cruises. The 2023 cruise also occurred during a period of La Niña but had a smaller MEI magnitude of -0.7 relative to the 2007 cruise. However, the 2023 La Niña event comes after three consecutive La Niña events in the years prior. Frequent periods of La Niña have provided favorable temperatures that increase gas solubility, which would increase dissolved CO_2 in the surface ocean. These consecutive La Niña events have the potential to compound DIC concentrations. Sutton et al. (2014) concluded that an increased frequency of La Niña events accompanied by more vigorous upwelling due to increased trade winds is indicative that the Equatorial Pacific has had a greater contribution of CO_2 to the atmosphere. Over the 30 years, an increase in DIC concentration was observed for most of the upper 1100 meters of the water column from 5N° to 5S° (Figure 8C). The highest ΔDIC was an increase of 200 μmol/kg at the surface. Below the thermocline, there was also a general increase in DIC concentration which could be a combination of anthropogenic carbon, strong upwelling during three consecutive moderates to stronger La Niña events, or elevated horizontal transport of water masses from other regions that are rich in carbon.

The ΔDIC between the three cruises indicates that water properties at the surface will fluctuate more than waters below the thermocline. Although speculative, the intuition that increased vertical transport of carbon-rich waters to the surface could be used to understand positive DIC anomalies during La Niña conditions, as seen in 2007 and 2023 (Mogollón, 2020). Although one can classify ENSO periods as either La Niña or El Niño, each event has different strengths and characteristics that may deviate from the average response (Mogollón, 2020). ENSO helps explain some of these fluctuations due to the changes in temperature and gas solubility; however, ENSO and seasonal variability are not the only contributors to the ΔDIC concentration during each cruise. One must also consider the anthropogenic factor that has contributed to increased CO_2 in the atmosphere (Figure 1). The ocean naturally wants to be in equilibrium with the atmosphere. Therefore, it will increase DIC concentration due to the uptake of anthropogenic carbon from the atmosphere (Sutton et al., 2014).

Anthropogenic Factor

Sabine et al. (2004) state that when anthropogenic CO_2 enters the ocean via the air-sea gas exchange, anthropogenic CO_2 concentrations are the highest in the near-surface. Most of the anthropogenic carbon that enters the ocean is confined to the thermocline, where the temperature changes quickly with increasing depth (Sabine et al., 2004). DIC concentrations for the three cruises support that the average surface DIC concentrations have a quasi-linear relationship with increased atmospheric CO_2 (Figure 9). The anthropogenic factor in the surface ocean is amplified by suitable conditions driven by ENSO and seasonal variability. In their study involving the (eMLR) method, Gruber et al. (2019), found that from 1994 to 2007, the Western equatorial Pacific had taken up to 14 μmol/kg of anthropogenic carbon in the upper 100 meters of the water column. This finding is consistent with Figure 8A, which suggests a total increased ΔDIC

ranging from 40 to 80 μmol/kg above the thermocline. According to Gruber et al. (2019), the anthropogenic signal is approximately 12 to 14 μmol/kg of that ΔDIC. The remaining increase in DIC from 1993 to 2007 may result from natural carbon sources.

Gruber et al. (2019) also concluded that the anthropogenic signal had reached as deep as 500 meters with an increase ranging from 2 μmol/kg to 10 μmol/kg of DIC below the thermocline. Although there are small regions of minimally increased ΔDIC in Figure 8A, the data from 1993 and 2007 suggest an overall decrease in DIC concentration below the thermocline for the given latitudes. This decrease in ΔDIC could result from increased primary production at depth or decreased upwelling rates from 1993 to 2007. A similar study involving the (eMLR) method would be helpful to assess how much the anthropogenic signal has changed from 2007 to 2023. The ΔDIC from 2007 to 2023 results from favorable conditions facilitated by ENSO and seasonal variability. This increase is in addition to the uptake of increased carbon resulting from human emissions.

Increasing the atmospheric anthropogenic carbon in the future could reverse changes in climate variability and help mask the anthropogenic signal rather than enhancing it (Sabine et al., 2008). Current climate models suggest that under climate change, the equatorial Pacific should expect to see increasing sea surface temperatures, weaker trade winds, and a shallower thermocline; however, there is not a clear path to determine how the intensity or frequency of ENSO events will be altered (Sutton et al., 2014). An estimated 90% of anthropogenic carbon is expected to be absorbed by the oceans on timescales of several thousand years; decadal studies suggest that the ocean may become less efficient as a sink for anthropogenic CO_2 (Sabine et al., 2004). Natural climate variability also prevents us from fully distinguishing between

anthropogenic contributions and decadal-climate variability, which can only be resolved by recorded long-term observations in the future (Landschützer et al., 2018).

Conclusion

This study suggests that the changes in DIC, in the Western Equatorial Pacific, over the 30 years correlate to seasonal changes, varying periods of ENSO, and increasing atmospheric CO_2. One limitation of this study is that the data measured did not have as much coverage over distance or depth relative to the cruises in 2007 and 1993. Other factors not considered in this study include primary production rates, nutrient availability, temperature, and upwelling rates, during each cruise. Any of the previously mentioned ocean properties could enhance or deplete the DIC concentration during each cruise. Continued study in this complex region contributes to our understanding of the natural and anthropogenic carbon dynamics and their impact on the delicate carbon balance of the ocean. Long-term records of this understudied region can help identify climate patterns and changes in future seasonal and ENSO variability resulting from human emissions.

Acknowledgements

I want to start by thanking the entire crew of the R/V Thomas G. Thompson for their outstanding seamanship and their accommodating welcoming to their vessel during a successful and safe voyage period. A special thanks to all the professors, from the School of Oceanography, for passing on their knowledge and wisdom of ocean dynamics and processes. I would also like to thank Graduate Student Ethan Campbell for his eagerness and dedication to teach and solve computer coding challenges that helped me convey my results in a manner that aligned with my initial vision. A special thanks to Assistant Professor Randie Bundy and Graduate Student Mary Margaret Stoll, who were instrumental in providing crucial feedback and assistance with data interpretation throughout the completion of my thesis. Thanks also to Associate Professor Mark Warner, who provided the necessary mentorship and flexibility that allowed me to narrow my thesis from the beginning of my capstone course and remain engaged until completion. Lastly, I would like to thank Professor and Director of the School of Oceanography, Rick Keil, for his passion for teaching students and his exemplary leadership, which I have benefited from academically and personally.

References

Bates, N.R., Y.M. Astor, M.J. Church, K. Currie, J.E. Dore, M. González-Dávila, L. Lorenzoni, F. Muller-Karger, J. Olafsson, and J.M. Santana-Casiano. (2014). *A time-series view of changing*
ocean chemistry due to ocean uptake of anthropogenic CO2 and ocean acidification. Oceanography 27(1):126–141, http://dx.doi.org/10.5670/oceanog.2014.16.

Carter, B. R., Feely, R. A., Wanninkhof, R., Kouketsu, S., Sonnerup, R. E., Pardo, P. C., et al. (2019). *Pacific anthropogenic carbon between 1991 and 2017.* Global Biogeochemical Cycles, 33, 597– 617. https://doi.org/10.1029/2018GB006154

Doney, S.C., Busch, S.D., Cooley, S.R., and Kroeker, K. J. (2020). *The Impacts of Ocean Acidification on Marine Ecosystems and Reliant Human Communities*. Retrieved from https://doi.org/10.1146/annurev-environ-012320083019

Gruber, N., Clement, D., Carter, B.R., Feely, R.A., Van Heuven, S., Hoppema, M., Ishii, M., Key, R.M., Kozyr, A., Lauvset, S.K., Monaco, C. L., Mathis, J.T., Murata, A., Olsen, A., Perez, F.F., Sabine, C.L., Tanhua, T., and Wanninkhof, R. (2019). *The oceanic sink for anthropogenic CO2 from 1994 to 2007. Science*363,1193-1199 (2019). DOI:10.1126/science.aau5153

Keeling, C. D., Brix, H., and Gruber, N. (2004). *Seasonal and long-term dynamics of the upper ocean carbon cycle at Station ALOHA near Hawaii.* Global Biogeochem. Cycles, 18, GB4006, doi:10.1029/2004GB002227.

Landschützer, P., Gruber, N., Bakker, D.C.E., Stemmler, I., and Six, K.D. (2018). *Strengthening seasonal marine CO_2 variations due to increasing atmospheric CO_2.* Nature Climate Change **8**, 146–150 (2018). https://doi.org/10.1038/s41558-017-0057-x

Lewis, E., & Wallace, D. (1998). *Program Devloped for CO {sub 2} system calculations*. Retrieved from https://doi.org/10.2172/639712

Merlivat, L., Boutin, J., Antoine, D., Beaumont, L., Golbol, M., and Vellucci, V. (2018). *Increase of dissolved inorganic carbon and decrease in pH in near-surface waters in the Mediterranean Sea during the past two decades*. Biogeosciences, 15, 5653–5662, https://doi.org/10.5194/bg-15-5653-2018, 2018.

Middelburg, J. J., Soetaert, K., and Hagens, M. (2020). *Ocean alkalinity,buffering and biogeochemical processes.* Reviews of Geophysics, 58,e2019RG000681. https://doi.org/10.1029/2019RG000681

Mogollón,R. (2020). *ENSO-driven CO2 efflux variability and the role of the upwelling region on the carbon exchange in the Northern Humboldt Current System.* Journal of Marine Systems, Volume 201,2020,103240,ISSN 0924-7963, https://doi.org/10.1016/j.jmarsys.2019.103240.

National Oceanic and Atmospheric Administration (NOAA). *Information on Batches of CO2 in Seawater Reference Material.* Retrieved from https://www.ncei.noaa.gov/access/ocean-carbon-acidification-data-system/oceans/Dickson_CRM/batches.html.

National Oceanic and Atmospheric Administration (NOAA). *Monthly Average Mauna Loa CO2.* Retrieved from https://gml.noaa.gov/ccgg/trends/

National Oceanic and Atmospheric Administration (NOAA). *Multivariate ENSO Index Version 2 (MEI.v2).* Retrieved from https://psl.noaa.gov/enso/mei/

Pimenta, A. R. and Grear J.S. (2018). *Guidelines for Measuring Changes in Seawater pH and Associated Carbonate Chemistry in Coastal Environment of Eastern United States.* Retrieved from https://www.epa.gov/sciencematters/guidelines-measuring-changes-seawater-ph

Sabine, C.L., Feely, R.A., Gruber, N., Key, R.M., Lee, K., Bullister, J.L., Wanninkhof, R., Wong, C.S., Wallace, D.W.R., Tilbrook, B., Millero, F.J., Peng, T.H., Kozyr, A., Ono, T., and Rios, A.F. (2004). *The oceanic sink for anthropogenic CO2.* Science Vol305, pages 367–371. (2004). DOI: 10.1126/science. 1097403

Sabine, C. L., Feely, R. A., Millero, F. J., Dickson, A. G., Langdon, C., Mecking, S., and Greeley, D. (2008). *Decadal changes in Pacific carbon.* J. Geophys. Res., 113, C07021, doi:10.1029/2007JC004577.

Sutton, A. J., R. A. Feely, C. L. Sabine, M. J. McPhaden, T. Takahashi, F. P. Chavez, G. E. Friederich, and J. T. Mathis (2014). *Natural variability and anthropogenic change in equatorial Pacific surface ocean pCO2 and pH.* Global Biogeochem. Cycles, 28, 131–145, doi:10.1002/2013GB004679.

Takahashi T., Sutherland S.C., Chipman D.W., Goddard J.G., Ho, C., Newberger T., Sweeney C., and Munro D.R. (2014). *Climatological distributions of pH, pCO2, total CO2, alkalinity, and CaCO3 saturation in the global surface ocean, and temporal changes at selected locations*. Marine Chemistry, Volume 164, 2014, Pages 95-125, ISSN 0304-4203, https://doi.org/10.1016/j.marchem.2014.06.004.